A LAIR-1 insertion creates broadly reactive antibodies against malaria variant antigens

Joshua Tan[1,2,3,*], Kathrin Pieper[1,*], Luca Piccoli[1,*], Abdirahman Abdi[2], Claire Maria Tully[2], Mathilde Foglierini Perez[1], Roger Geiger[1,5], David Jarrossay[1], Francis Maina Ndungu[2], Juliana Wambua[2], Philip Bejon[2,3], Chiara Silacci Fregni[1], Blanca Fernandez-Rodriguez[1], Sonia Barbieri[1], Siro Bianchi[4], Kevin Marsh[2,3], Vandana Thathy[2], Davide Corti[4], Federica Sallusto[1], Peter Bull[2,3,$] and Antonio Lanzavecchia[1,5,$]

[1]Institute for Research in Biomedicine, Università della Svizzera Italiana, Via Vincenzo Vela 6, 6500 Bellinzona, Switzerland

[2]KEMRI-Wellcome Trust Research Programme, CGMRC, PO Box 230, 80108 Kilifi, Kenya

[3]Nuffield Department of Clinical Medicine, University of Oxford, John Radcliffe Hospital, Headington, Oxford, OX3 9DU, UK

[4]Humabs BioMed SA, 6500 Bellinzona, Switzerland

[5]Institute for Microbiology, ETH Zurich, Wolfgang-Pauli-Strasse 10, 8093 Zurich, Switzerland

*[$]These authors contributed equally to this work

Correspondence: lanzavecchia@irb.usi.ch and PBull@kemri-wellcome.org

Abstract

Plasmodium falciparum antigens expressed on the surface of infected erythrocytes are important targets of naturally acquired immunity, but their high number and variability provide the pathogen with a powerful means of escape from host antibodies. Although broadly reactive antibodies against these antigens could be useful as therapeutics and in vaccine design, their identification has proven elusive so far. Here, we report the isolation of human monoclonal antibodies that recognize erythrocytes infected by different *P. falciparum* isolates and opsonize these cells by binding to members of the RIFIN family. These antibodies acquired broad reactivity through a novel mechanism of DNA insertion between the V and DJ segments. The insert, which is necessary and sufficient for binding to RIFINs, is the collagen-binding domain of LAIR-1, an Ig superfamily inhibitory receptor encoded on chromosome 19. In each of the two donors studied, the antibodies are encoded by a single expanded B cell clone and carry distinct mutations that abolish binding to collagen and increase binding to infected erythrocytes. These findings illustrate, with a biologically relevant example, a novel mechanism of antibody diversification and demonstrate the existence of accessible and conserved epitopes that may be suitable candidates for the development of a malaria vaccine.

Introduction

Plasmodium falciparum is the causative agent of the most deadly form of malaria and accounts for 600,000 deaths yearly[1]. During the blood stage of its life cycle, *P. falciparum* expresses and inserts proteins into the membranes of erythrocyte host cells, modifying their cytoadhesive and immunological properties[2]. Many of these proteins belong to large families collectively known as variant surface antigens (VSAs), of which the best-characterized are *P. falciparum* erythrocyte membrane protein-1 (PfEMP1), repetitive interspersed family (RIFIN) proteins and sub-telomeric variable open reading frame (STEVOR) proteins[3]. VSAs are thought to play a role in malaria pathology by promoting binding of infected erythrocytes (IE) to uninfected erythrocytes to form rosettes, and by mediating adhesion of IE to endothelial cells, which leads to

sequestration of IE in various organs[2,4,5]. Following natural exposure, VSAs stimulate an antibody response that develops progressively and contributes to naturally acquired immunity[6-8]. This immunity takes several years to develop because *P. falciparum* is able to evade the host response through clonal antigenic variation[9,10]. Indeed, sera from adults who have grown up in malaria endemic areas and are protected from clinical disease recognize many parasite isolates[11,12]. The broad reactivity of the sera is thought to be predominantly due to a large repertoire of variant-specific antibodies[13], but a rigorous search for broadly reactive antibodies against VSAs[11,13,14] has yet to be conducted.

Results

Isolation of monoclonal antibodies that broadly bind to infected erythrocytes

To identify individuals that may produce broadly reactive antibodies, we developed an improved mixed agglutination assay[13] **(Fig. 1a)**. Plasma from adults (n = 557) living in a malaria-endemic region in Kilifi, Kenya, were initially tested in pools of five (**Fig. 1b**) and then individually for their capacity to agglutinate mixtures of erythrocytes infected with three culture-adapted Kenyan parasite isolates, each stained with a different DNA dye (a total of nine isolates tested). Most plasma samples formed single-colour agglutinates, but three were able to form mixed-colour agglutinates with at least six isolates (**Fig. 1c**). A single isolate (10668) was not detected in mixed agglutinates formed by any of the plasma and was therefore excluded from the study.

From two selected donors (coded C and D) whose plasma formed mixed agglutinates with at least eight isolates, we immortalized IgG^+ memory B cells using an established protocol[15] and screened the culture supernatants for their capacity to stain erythrocytes infected with the eight isolates. Surprisingly, most antibodies isolated from these donors stained multiple isolates, with the best antibodies, such as MGC34, MGD21 and MGD39, recognizing all eight isolates tested (**Fig. 1d**). Conversely, a few antibodies, such as MGD13, were specific for a single isolate. In all cases, only a fraction of IE was stained (**Fig. 1e)** and this fraction varied with different antibodies, possibly reflecting different affinities of the antibodies or different expression levels of the antigens. Overall,

these findings show that broadly reactive antibodies against VSAs can be generated in response to malaria infection.

Broadly reactive antibodies contain mutated LAIR-1 inserts

We investigated the molecular basis of the broad antibody reactivity by comparing the sequences of the antibodies isolated from the two donors. While the antibodies with narrow reactivity showed classical VDJ organization of the heavy (H) chain gene, all the broadly reactive antibodies (14 from donor C, 13 from donor D) carried a large insert of more than 100 amino acids between their V and DJ segments (**Fig. 2a and Extended Data Fig. 1-2**). In both donors, the core of the inserts encoded an amino acid sequence that was 92-98% homologous to the extracellular domain of LAIR-1, a collagen-binding inhibitory receptor encoded in the leukocyte receptor locus on chromosome 19 (Chr19)[16]. However, in each donor, the broadly reactive antibodies used a distinct VH/JH combination (VH3-7/JH6 in donor C and VH4-4/JH6 in donor D) and had junctions of distinct length between the V, LAIR-1 and J segments. In addition, the broadly reactive antibodies from donor D shared a single light (L) chain (VK1-8/JK5), while the antibodies from donor C had one of three different L chains (VK1-5/JK2, VK4-1/JK2, VL7-43/JL3) (**Extended Data Fig. 3**).

All the broadly reactive antibodies carried a high load of somatic mutations spanning the whole V-LAIR-1-DJ region. The mutations in the VH were used to reconstruct genealogy trees showing a developmental pathway with progressive acquisition of somatic mutations (**Fig. 2b-c**). Notably, the trees were consistent with those generated using only the LAIR-1 insert or the VL sequence (**Extended Data Fig. 4**).

Collectively, the above findings indicate that, within each individual, a single B cell clone carrying a LAIR-1 insert was expanded following stimulation by malaria antigens and progressively accrued mutations in LAIR-1, VH and VL regions.

Genomic structure of the LAIR-1 insert

To address the mechanism that led to the generation of the LAIR-1-containing antibodies, we compared cDNA and genomic DNA sequences obtained from the antibody-producing B cell clones **(Fig. 3)**. In both donors, the genomic DNA contained a LAIR-1 insert that was larger than that found in the corresponding cDNA. In particular, in donor C, the insert comprised not only the 291 bp exon encoding the extracellular LAIR-1 domain, but also a 194 bp 5' intronic region of the LAIR-1 gene that was partially spliced out in the mRNA, and a shorter 23 bp 3' intronic region that was maintained in the mRNA (**Extended Data Fig. 5)**. Donor D had a somewhat different genomic insertion, with larger 5' (378 bp) and 3' (60 bp) LAIR-1 intronic sequences, and, 5' of the LAIR-1 insertion, an additional sequence of 138 bp corresponding to an intergenic sequence of Chr13 **(Extended Data Fig. 6)**. In this donor, the entire LAIR-1 5' intronic sequence and much of the 5' Chr13 sequence were spliced out in the mRNA.

To gain insight on the mechanism leading to the insertion of LAIR-1, we analysed the sequences flanking the LAIR-1 and Chr13 inserts. We identified cryptic recombination signal sequences (RSSs) that followed the 12/23 rule but had poor RSS prediction scores and were not positioned precisely at the ends of the inserts **(Extended Data Fig. 7)**. In addition, the inserts were located exactly between V and D/J segments and were joined to these segments by N-nucleotides. These findings would be consistent with single or multiple RAG-dependent DNA transposition events followed by selective splicing leading to the expression of a functional protein.

The mutated LAIR-1 domain is necessary and sufficient for binding to IE

To determine the contribution of the mutated VH, VL and LAIR-1 domains to the antibody specificity, we generated a panel of constructs and fusion proteins based on the broadly reactive antibody MGD21 (**Fig 4a**). Substitution of the V, J or L chain of MGD21 with that of an unrelated antibody did not affect binding to IE, suggesting that these elements are dispensable for binding (**Fig. 4b**). In contrast, deletion of the LAIR-1 insert, or its reversion to the unmutated genomic sequence, led to a complete loss of

binding. Furthermore, fusion proteins displaying only the mutated LAIR-1 exon with or without flanking sequences showed specific binding to IE, although with lower affinity.

To understand the contribution of the somatic mutations of the LAIR-1 insert to antigen binding, we created a set of LAIR-1-Fc fusion proteins carrying, in various combinations, the mutations shared by MGD21 with other antibodies of the same clonal family. We tested the mutants for binding to IE and to collagen, which is the natural ligand of LAIR-1. Interestingly, two distinct kinds of mutations were identified: those that reduced collagen binding and those that increased binding to IE (**Fig. 4c, d**). In particular, a single mutation (P107R) was sufficient to abrogate collagen binding, while three mutations (T67L, N69S and A77T) synergized in promoting binding to IE.

Taken together, these findings indicate that the binding of the broadly reactive antibodies to IE relies mainly on the mutated LAIR-1 domain, which evolves under selective pressure to lose collagen binding and gain binding to IE.

LAIR-1-containing antibodies bind to distinct members of the RIFIN family

To facilitate the identification of the antigen(s) recognized by the LAIR-1-containing antibodies, we used the fully sequenced *P. falciparum* 3D7 strain and isolated stable parasite lines that were enriched (3D7-MGD21^{+}) or depleted (3D7-MGD21^{-}) of MGD21 reactivity (**Fig. 5a**). Western blot analysis showed two MGD21-reactive bands of 40-45 kDa in ghosts and in MGD21 immunoprecipitates (IP) prepared from 3D7-MGD21^{+} IE (**Fig. 5b**). These bands were absent in control samples prepared from 3D7-MGD21^{-} IE ghosts or from those immunoprecipitated with an irrelevant antibody.

Analysis of the IP using liquid chromatography-coupled mass spectrometry (LC-MS) revealed that a member of the A-type RIFIN family (PF3D7_1400600) was significantly enriched in IP obtained with MGD21 as compared to IP obtained with a control antibody (Log_2 fold change >2; $P < 0.01$) (**Fig. 5c**). PF3D7_1400600, as well as a second A-type RIFIN (PF3D7_1040300), was also identified by LC-MS in 3D7-MGD21^{+} but not in 3D7-MGD21^{-} ghosts in the absence of immunoprecipitation **(Fig. 5d)**. The MW of these two RIFINs (41 and 42 kDa) and their degree of enrichment were consistent with the two bands observed in the Western blot. Notably, four other RIFINs,

including one recently characterized for its capacity to induce rosetting (PF3D7_0100400)[5], were detected in similar amounts by LC-MS in both 3D7-MGD21$^+$ and 3D7-MGD21$^-$ ghosts.

We found that enrichment for 3D7-MGD21$^+$ IE greatly increased recognition by all the other broadly reactive antibodies from donor D tested and, notably, by two broadly reactive antibodies from donor C, suggesting that these antibodies recognize the same antigens **(Extended Data Fig. 8)**. The binding of the LAIR-1-containing antibodies to specific RIFINs was confirmed by the finding that MGD21 stained CHO cells transfected with the candidate antigens (PF3D7_1400600 and PF3D7_1040300), but not with irrelevant RIFINs that were similarly expressed (PF3D7_0100400 and PF3D7_0100200) or not detected (PF3D7_1100500) in 3D7-MGD21$^+$ and 3D7-MGD21$^-$ ghosts (**Fig. 5e and Extended Data Fig. 8**). PF3D7_1400600- or PF3D7_1040300-transfected CHO cells were also stained by most of the antibodies that stained 3D7-MGD21$^+$ IE, but not by those that failed to stain the parasite line.

To investigate whether the LAIR-1-containing antibodies also recognize RIFINs expressed by the Kenyan isolates (e.g. 9605), we repeated the immunoprecipitation assay with 9605-MGD21$^+$ and 9605-MGD21$^-$ IE. Western blot analysis revealed two MGD21-reactive bands in 9605-MGD21$^+$ samples with the expected molecular weight (**Extended Data Fig. 9a**). Furthermore, enrichment for 9605-MGD21$^+$ IE greatly increased binding by all the MGC and MGD antibodies tested (**Extended Data Fig. 9b**), suggesting that these antibodies (including those that do not bind to 3D7 RIFINs) recognize RIFINs expressed by isolate 9605. Collectively, these results indicate that the LAIR-1-containing antibodies recognize specific members of the RIFIN family in different *P. falciparum* isolates.

Addition of MGD21 to 3D7 culture did not interfere with parasite growth and did not result in decreased expression of the antigen(s) (**Extended Data Fig. 10a-b**). In addition, when tested in a rosette inhibition assay with O$^+$ or A$^+$ erythrocytes, MGD21 did not show a consistent inhibitory effect (P = ns for both blood groups) (**Extended Data Fig. 10c**). In contrast, MGD21 showed a strong capacity to opsonize 3D7 IE for phagocytosis by human monocytes **(Fig. 5f)**. Opsonization was dependent on an intact Fc, as a mutant lacking Fc receptor binding (MGD21 LALA) did not induce phagocytosis. Similar results were obtained with other broadly reactive antibodies

isolated from both donors and with a different parasite isolate (11019) (**Extended Data Fig. 10d**), suggesting that these broadly reactive antibodies could be effective in promoting phagocytosis and destruction of IE *in vivo*.

Discussion

Our study reveals a new mechanism of diversification that leads to the generation of potent and broadly reactive antibodies that bind to RIFINs on erythrocytes infected with different *P. falciparum* isolates. These findings open several questions as to the potential use of RIFINs as targets for passive and active vaccination and as to the general relevance of the mechanism of DNA transposition that generated these broadly reactive antibodies.

Broad recognition of RIFINs by LAIR-1-containing antibodies

RIFINs represent the largest family of VSAs, with as many as 150 polymorphic genes, some of which have been recently implicated in severe *P. falciparum* malaria[5]. RIFINs are expressed at multiple stages in the parasite life cycle[17,18] and have been shown to generate an antibody response following natural infection[19]. The LAIR-1-containing antibodies bind to RIFINs on intact IE and have potent opsonizing activity, which would be consistent with their role in decreasing the burden of IE *in vivo* by enhancing parasite clearance in the spleen. The staining of only a fraction of IE by the LAIR-1-containing antibodies is consistent with the clonal expression of RIFINs[5] and suggests that these antibodies may not be sufficient to take full control of the infection. Nevertheless, given the fact that *in vitro* cultured parasites downregulate and sometimes lose VSA expression due to the lack of selection pressure[20], it is difficult to extrapolate these *in vitro* results to the *in vivo* setting. In particular, it will be important to determine whether the parasites that escape from antibody recognition maintain virulence *in vivo*. It will also be interesting to determine whether the LAIR-1-containing antibodies recognize the RIFINs that are expressed at other stages of the parasite life cycle, such as sporozoites, merozoites and gametocytes[17,18].

In the context of vaccine development, it is encouraging to find conserved epitopes present on a large fraction of IE from multiple and possibly all parasite isolates. It remains to be established whether the conserved RIFIN epitopes identified by the LAIR-1-containing antibodies could also be recognized by conventional antibodies and whether this antibody response would have sufficient breadth to control disease and possibly transmission. Immunoepidemiological studies and controlled human experimental infections[21] may help to assess the potential of the RIFIN-based approach for serotherapy and vaccine design.

A new mechanism of antibody diversification

The unusual architecture of the LAIR-1-containing antibodies illustrates a novel mechanism of inter-chromosomal DNA transposition that can contribute to antibody diversification. The presence of cryptic 12/23 RSSs and N-nucleotides at the ends of the LAIR-1 and Chr13 inserts suggests that V(D)J recombinase was involved in the excision of the DNA fragments. Indeed, RAG1/2 preferentially binds to transcriptionally active sites[22] and LAIR-1 is transcribed in developing B cells[23]. We postulate that these fragments, which are comparable to signal joints, are rejoined into the resolving coding ends of a V-DJ locus[24,25]. V(D)J recombinase is primarily active in developing B cells, but can also be reactivated in germinal center B cells[26] and has been implicated in inter-chromosomal genomic rearrangements at cryptic RSSs outside the Ig and TCR loci[27,28], and in the formation of chromosomal translocations found in human lymphomas[29,30]. Nevertheless, we cannot exclude that the production of LAIR-1-containing antibodies might be the consequence of AID-dependent genomic instability caused by chronic *Plasmodium* infection, as recently demonstrated in a mouse model[31].

The transposition of LAIR-1 (and Chr13) sequences into rearranging V-DJ genes is the first example of an insertion that gives rise to a functional antibody where the insert represents the fundamental binding element. We propose that in the two donors studied, a rare somatic event generated a single B cell clone that expanded under selective pressure to lose collagen reactivity and to increase binding to the RIFINs present in the parasite population. The large expansion of the clones and the extraordinary degree of intraclonal

diversification could be the consequence of continuous stimulation by variable parasites encountered over a period of several years. It is tempting to speculate that, due to the strong reactivity of LAIR-1 for collagen, the pre-B cell would be forced to edit the BCR[32], which may explain the presence of three different light chains in clones from donor C. However, given that in this case the self reactivity is uniquely encoded by the LAIR-1 insert, the only way to escape would be through somatic mutation of this domain[33], and we have indeed identified mutations that reduce collagen binding.

It remains to be established how often this novel mechanism may give rise to functional antibodies and whether sequences other than LAIR-1 are transposed into rearranging Ig genes. The mechanism of DNA transposition between V and DJ leading to its expression in the CDR3 loop offers the possibility to accommodate different protein domains in the antibody structure with minimal disruption, while splicing offers the further advantage of maintaining the boundaries of a protein domain.

In the specific case of the two donors studied, the large expansion of LAIR-1 positive clones can be attributed to the fact that these donors were chronically exposed to malaria and that LAIR-1 is a good substrate to generate a RIFIN-binding domain through just a few mutations, as we have shown. The finding that the unmutated LAIR-1 domain does not bind to RIFINs is intriguing and is reminiscent of what is found in broadly neutralizing anti-HIV antibodies of the VRC01 class, which do not bind when reverted to their unmutated forms[34]. We anticipate that other cases of LAIR-1-containing antibodies will be found in malaria-endemic regions, but similar clones are unlikely to emerge in malaria-free countries, although we speculate that such clones may be recruited in an anti-collagen response that is characteristic of certain rheumatic diseases[35].

Figure legends

Figure 1. Identification of broadly reactive monoclonal antibodies against IE. a, Fluorescence microscopy images of single agglutinates (top) and a triple agglutinate (bottom). **b-c,** Plasma (pooled in groups of five) from immune adults were screened against six parasite isolates using the triple mixed agglutination assay (**b**). Pools that formed mixed agglutinates with at least five isolates (in red) were further investigated for individual reactivity against an extended panel of 8 isolates (**c**). **d,** Heat map showing the percentage of IE of eight parasite isolates stained by monoclonal antibodies isolated from two donors. Closely related antibodies are grouped in alternating colors. n = 1 **e,** Example of staining of IE by the broadly reactive antibody MGD55.

Figure 2. Broadly reactive antibodies contain a mutated LAIR-1 insert and are produced by expanded clones. a, Protein sequence alignment of MGC1 and MGD21 with germline-encoded sequences of the corresponding VH (green or purple), DH (cyan), JH (blue) and LAIR-1 (exon in red and intronic sequences in light red). Chr13 sequences are shown in orange while junctions are shown in grey. **b-c,** Genealogy trees drawn from the VH nucleotide sequences of antibodies from donors C **(b)** and D (**c**). In the donor C genealogy tree, antibodies that use different light chains are highlighted in different colours. Shown are the nucleotide and amino acid substitutions, with the latter in parentheses.

Figure 3. Genomic and cDNA structure of the LAIR-1 inserts. Scheme showing genomic DNA and cDNA of LAIR-1-containing antibodies from donors C and D. Shown are the lengths of the fragments (bp in parentheses), cryptic 12/23 RSS sites (triangles) and splicing positions (dashed lines).

Figure 4. The mutated LAIR-1 insert is necessary and sufficient for binding to IE. a, Design of modified MGD21 antibody constructs with selected regions replaced with counterparts from an unrelated antibody (FI499) [C1-C2, C9], deleted [C3-C6], or reverted to germline (GL) [C7-C8]. Fc fusion proteins that incorporated the LAIR-1 insert, junction and downstream sequences [F1], as well as the LAIR-1 exon alone [F2],

were also designed. **b,** Binding of MGD21 constructs and Fc fusion proteins to IE. One representative of n = 2 independent experiments. **c-d**, Selected amino acid substitutions found in MGD21 were added individually or in different combinations to the germline LAIR-1-Fc fusion protein. These mutants were tested for binding to collagen and to IE. Shown are the effect of the mutations on binding to IE or collagen (one representative of n = 2 independent experiments) (**c**) and their location on the LAIR-1 structure[36] (pdb, 3kgr) (**d**). Gain of IE binding is shown in green (background mean fluorescence intensity (MFI) values subtracted). Loss of collagen binding (EC50 ELISA values) is shown in red.

Figure 5. LAIR-1-containing antibodies bind to distinct RIFINs and opsonize IE. a, MGD21 staining of 3D7 IE that were enriched or depleted of MGD21 reactivity. n = 3 independent experiments. **b,** Western blot showing MGD21 binding to erythrocyte ghosts and MGD21 IP prepared from 3D7-MGD21^{+} and 3D7-MGD21^{-} IE. Controls include uninfected erythrocytes (uE) and IP with an irrelevant antibody (BKC3). Specific bands are marked with stars. Anti-human IgG was used as secondary antibody, resulting in detection of antibodies used for IP alongside antigens of interest. n = 2 independent experiments. **c**, Volcano plot from LC-MS analysis of MGD21 versus BKC3 IP prepared from 3D7-MGD21^{+} IE. n = 4 independent experiments. **d,** Heat map from LC-MS analysis showing RIFIN expression levels (calculated as iBAQ scores[37,38]) in erythrocyte ghosts prepared from 3D7-MGD21^{+} and 3D7-MGD21^{-} IE. Grey boxes indicate that expression levels are below the detection limit. **e,** MGD21 and BKC3 staining of CHO cells transfected with a specific (PF3D7_1400600) or an irrelevant (PF3D7_0100200) RIFIN. n = 5 independent experiments. **f,** Opsonic phagocytosis of 3D7-MGD21^{+} IE by monocytes. The IE were stained with DAPI, which was quantified in monocytes as a measure of phagocytosis. n = 2 for MGD21, MGD21 LALA, BKC3, n = 1 for others.

Extended Data Figure 1. Nucleotide sequence alignments of VH regions of antibodies isolated from donors C (a) and D (b). Dots indicate positions where the nucleotide of a mature antibody is identical to that of the UCA.

Extended Data Figure 2. Protein sequence alignments of VH regions of antibodies isolated from donors C (a) and D (b). Putative complementarity-determining regions (CDRs) are highlighted in red. Dots indicate positions where the amino acid of a mature antibody is identical to that of the UCA.

Extended Data Figure 3. Nucleotide sequence alignments of VL regions of antibodies isolated from donors C (a-c) and D (d). Complementarity-determining regions (CDRs) are highlighted in red. Dots indicate positions where the nucleotide of a mature antibody is identical to that of the UCA.

Extended Data Figure 4. Genealogy trees generated from VL and LAIR-1 exon sequences. The trees were drawn based on the somatic mutations in light chain variable regions **(a, b)** or LAIR-1 exons **(c, d)** of the antibodies isolated from donors C and D. In the donor C VL trees, VL(1), VL(2) and VL(3) refer to VL7-43/JL3, VK1-5/JK2 and VK4-1/JK2, respectively. Shown are the nucleotide and amino acid substitutions, with the latter in parentheses.

Extended Data Figure 5. The LAIR-1 intron is partially spliced out in mature antibody mRNA. The sequence alignment of genomic DNA (gDNA) and cDNA of antibody MGC28 reveals a 507 bp LAIR-1 insert in Chr14 and the removal of a 160 bp fragment 5' of the LAIR-1 exon by RNA splicing. Splice donor and acceptor sites are highlighted in yellow.

Extended Data Figure 6. Genomic DNA analysis reveals a Chr13 insertion in LAIR-1-containing antibodies of donor D. Shown is an alignment of a region of antibody-encoding DNA (Chr14) with the corresponding region of Chr13 from gDNA isolated

from B cells of clone MGD19. The sequence maintained in the mature antibody mRNA is boxed and the splice donor site is highlighted in yellow.

Extended Data Figure 7. LAIR-1 and Chr13 inserts in antibodies are flanked by 12/23 cryptic RSS sites. The regions on Chr19 and Chr13 of donor-derived genomic DNA corresponding to the ends of the inserts were sequenced and RSS sites were identified using the RSSsite web server. The sequences shown begin from the ends of the inserts. Cryptic RSS sites are highlighted in grey, with complementary ends underlined and prediction scores shown in parentheses.

Extended Data Figure 8. Reactivity of representative MGC and MGD antibodies to 3D7 IE and 3D7 RIFIN-transfected CHO cells. Shown is the percentage of IE (one representative of n = 2 independent experiments) or of transfected CHO cells (n = 1) stained by the antibodies. RIFINs that were enriched in 3D7-MGD21^{+} ghosts are highlighted blue, while RIFINs that were similarly expressed or not detected in 3D7-MGD21^{-} and 3D7-MGD21^{+} ghosts are shown in red. BKC3 is a negative control antibody.

Extended Data Figure 9. Reactivity of MGC and MGD antibodies to the Kenyan parasite isolate 9605. a, Western blot showing MGD21 binding to IP prepared from 9605-MGD21^{-} and 9605-MGD21^{+} IE. Specific bands are marked with a star. Anti-human IgG was used as secondary antibody, resulting in detection of antibodies used for IP alongside antigens of interest. n = 2 independent experiments. **b,** Percentage of 9605-MGD21^{-} and 9605-MGD21^{+} IE recognized by representative MGC and MGD antibodies. BKC3 is a negative control antibody. One representative of n = 2 independent experiments.

Extended Data Figure 10. Functional assays of LAIR-1-containing antibodies. a, Parasitemia of 3D7-MGD21^{+} *in vitro* culture after 2 d of incubation with various concentrations of MGD21 or an irrelevant antibody (BKC3). n = 1. **b,** Percentage of 3D7-MGD21^{+} IE recognized by MGD21 after 2 d of incubation with various concentrations of MGD21 or BKC3. The antibodies were removed after 2 d (during the ring stage of the

life cycle) and the parasites were allowed to grow for 24 h to the late trophozoite/schizont stage prior to detection with MGD21. n = 1. **c,** Rosetting of 9605-MGD21^{+} IE with blood group O^{+} or A^{+} uninfected erythrocytes (uE) after incubation with MGD21 or BKC3. Mean ± SD of n = 4 independent experiments. **d,** Opsonic phagocytosis of 11019-MGD21^{+} IE by monocytes. The IE were stained with DAPI, which was quantified in monocytes as a measure of phagocytosis. n = 1.

Methods

Parasite culture and selection. The *Plasmodium falciparum* clone 3D7 and nine laboratory-adapted parasite isolates from severe and non-severe malaria patients in Kilifi, Kenya (sampled between 2009 and 2010), were cultured *in vitro* according to standard procedures[39] and cryopreserved at the late trophozoite stage for use in subsequent assays. To select for MGD21-reactive infected erythrocytes (IE), cultured IE were incubated with MGD21 for 20 min at room temperature, washed, and rotated with Protein G-coated magnetic beads (Life Technologies) for 30 min at room temperature. Following magnetic sorting, enriched ($MGD21^+$) and depleted ($MGD21^-$) fractions were returned to *in vitro* culture.

Triple mixed agglutination assay. Following informed consent, plasma samples were taken from 2007 to 2014 from 557 adults living in a malaria-endemic region within Kilifi County on the coast of Kenya. The study was approved by the Kenya Medical Research Institute Ethics Review Committee and the Oxford Tropical Research Ethics Committee. IE from three parasite isolates were separately stained with 10 μg/mL DAPI, 200 μg/mL ethidium bromide or 6.7× SYBR Green I for one hour at room temperature. The stained parasites were washed five times, mixed in equal proportions, and diluted to a 5% haematocrit in incomplete RPMI medium. Ten μL of the parasite mixture was rotated with 2.5 μL of adult plasma for 1.5 h at room temperature, and agglutinates formed were examined by fluorescence microscopy. In the primary screen, pools of five adult plasma were tested against six Kenyan isolates (in two separate reactions). Pools that formed mixed-colour agglutinates were identified and individual plasma within these pools were tested against nine isolates using the same assay. Two adults with plasma that formed mixed agglutinates with eight parasite isolates were selected for monoclonal antibody isolation and, following further informed consent, an additional blood sample was taken from each individual in February 2014.

B cell immortalization and isolation of monoclonal antibodies. IgG^+ memory B cells were isolated from cryopreserved PBMCs by magnetic cell sorting with mouse anti-CD19-PECy7 antibodies (BD Pharmingen, order number 341113) and mouse anti-PE

microbeads (Miltenyi Biotec, order number 130-048-081), followed by flow cytometry sorting for IgG^+ IgM^- IgD^- cells. The B cells were immortalized with Epstein–Barr virus (EBV) in the presence CpG-DNA (2.5 μg/mL) and irradiated feeder cells as described previously[15]. Two weeks post-immortalization, culture supernatants were tested for the ability to stain IE from eight parasite isolates by flow cytometry. Cryopreserved IE were thawed, stained with 10× SYBR Green I, and incubated with the B cell supernatants for 1 h at 4ºC. Antibody binding was detected using 2.5 μg/mL of goat Alexa Fluor 647-conjugated anti-human IgG (Jackson ImmunoResearch, order number 109-056-098). Reactivity was calculated based on the percentage of late-stage parasites (high SYBR Green) recognized by each antibody.

Sequence analysis of antibody cDNA and genomic DNA. cDNA was synthesized from selected B cell cultures and both heavy chain and light chain variable regions (VH and VL) were sequenced as previously described[40]. The usage of VH and VL genes and the number of somatic mutations were determined by analyzing the homology of VH and VL sequences of mAbs to known human V, D and J genes in the IMGT database[41]. Genomic DNA was isolated from the B cell lines with a commercial kit (QIAGEN), and antibody-encoding sequences were amplified and sequenced with primers specific for the V and J regions of the given antibody. Sequences were aligned with ClustalW2[42]. Potential cryptic RSS sites were identified using the RSSsite web server[43].

Immunoglobulin lineage and genealogy analysis. Unmutated common ancestor (UCA) sequences of the VL were inferred with Antigen Receptor Probabilistic Parser (ARPP) UA Inference software, as previously described[44]. UCA sequences of the VH were constructed using IMGT/V-QUEST[41] and the genomic insert sequences. Nucleotide sequences of the mutated antibodies and the UCA were aligned using ClustalW2[42], and phylogenetic trees were generated with the DNA Maximum Likelihood program (Dnaml) of the PHYLIP package, version 3.69[45,46].

Production of recombinant antibodies, antibody variants and fusion proteins. Antibody heavy and light chains were cloned into human IgG1, Igκ and Igλ expression vectors[40] and expressed by transient transfection of Expi293F Cells (ThermoFisher Scientific) using polyethylenimine (PEI). Cell lines were routinely tested for mycoplasma

contamination. The antibodies were affinity purified by protein A chromatography (GE Healthcare). Variants of the MGD21 antibody were produced by i) exchanging V_H, D_H, J_H elements or the light chain with the corresponding sequences of an irrelevant antibody (FI499, reactive to influenza virus[46]), ii) deleting selected segments, or iii) reverting somatic mutations to the germline configuration with reference to the IMGT database and the original LAIR-1 genomic sequence (NCBI Reference Sequence: NC_018930.2). In addition, LAIR-1-Fc fusion proteins were produced recombinantly by cloning the mutated or unmutated LAIR-1 fragment into a plasmid designed for expression of human IgG1 fusion proteins (pINFUSE-hIgG1-Fc2, Invivogen). Based on an alignment of the most potent LAIR-1-containing antibodies with the unmutated LAIR-1 sequence, five key residues that could contribute to gain of binding to IE and loss of binding to collagen were identified and added alone or in various combinations to the unmutated LAIR-1-Fc fusion protein. The MGD21 constructs and LAIR-1 exon mutants were tested for staining of 3D7 IE that were enriched for MGD21 recognition (3D7-MGD21$^+$). For the LAIR-1 exon mutants, MFI values at 1 μg/mL antibody concentration were calculated by interpolation of binding curves fitted to a linear regression model (Graphpad Prism 6).

ELISA. Total IgGs were quantified using ELISA plates coated with goat anti-human IgG (SouthernBiotech, order number 2040-01) using Certified Reference Material 470 (ERMs-DA470, Sigma-Aldrich) as a standard. Binding to human collagen type I was tested by ELISA using 96-well MaxiSorp plates (Nunc). Briefly, ELISA plates were coated with 5 μg/mL of type I recombinant human collagen (Millipore, order number CC050), blocked with 1% BSA and incubated with titrated antibodies, followed by AP-conjugated goat anti-human IgG, Fcγ fragment specific (Jackson Immuno Research, order number 109-056-098). Plates were then washed, substrate (p-NPP, Sigma) was added and plates were read at 405 nm.

Immunoprecipitation and LC-MS. Erythrocyte ghosts were prepared by hypotonic lysis with 1× PBS diluted 15-fold in water, and ghost membranes were dissolved in a reducing lysis buffer containing 2% SDS, 10 mM DTT, 10 mM HEPES pH 8, sonicated and boiled. Solubilized proteins were alkylated with iodoacetamide (final concentration 55 μM) for 30 min at room temperature and precipitated with 80% acetone overnight at 4ºC. The precipitates were resuspended in urea and digested with trypsin. For

immunoprecipitation experiments, IE were sonicated and dissolved in 7.2 M urea in RIPA buffer (1% Triton X-100, 0.1% SDS, 0.5% sodium deoxycholate in HBS pH 7.4). The samples were centrifuged and supernatants were diluted 6.7-fold with RIPA buffer containing a protease inhibitor cocktail (Sigma-Aldrich) and incubated with 10 μg of MGD21 or BKC3 overnight at 4ºC. Next, Protein G-Sepharose beads (GE Healthcare) were added and samples were incubated for 1 h at 4ºC. The beads were washed four times and immunoprecipitates were digested directly on the beads with trypsin. After trypsin digestion, peptides were analyzed on a Q-Exactive instrument at the Functional Genomics Center in Zürich. Raw files were analyzed using the MaxQuant software[37] and MS/MS spectra were searched against the human and *P. falciparum* 3D7 UniProt FASTA databases. Peptide identifications were matched across several replicates. Subsequent data analysis was performed in the R statistical computing environment. Missing values were imputed with a normal distribution around an LFQ value of 21. Statistical significance was evaluated by Welch tests.

Western blots. Ghosts and immunoprecipitates were dissolved in 2× SDS sample buffer (Bio-Rad) and run on a 12% polyacrylamide gel under non-reducing conditions. The proteins on the gel were transferred onto a PVDF membrane, which was blocked with 5% milk in TBS with 0.1% Tween (TBST) for 1 h at room temperature. The membrane was incubated with 5 μg/mL MGD21 overnight at 4ºC, washed with TBST, and developed with HRP-conjugated sheep anti-human IgG (GE Healthcare, order number NA933) used in combination with a chemiluminescent substrate.

Expression of RIFINs. Genes encoding the A-RIFINs PF3D7_1400600, PF3D7_1040300, PF3D7_0100400, PF3D7_0100200, and PF3D7_1100500 were produced by gene synthesis (Genscript) and cloned into the pDisplay vector (Invitrogen), which contains an HA tag, as previously described[5]. The pDisplay constructs were transiently transfected into CHOK1-SV cells (GS-System, Lonza) using PEI. Cell lines were routinely tested for mycoplasma contamination. Briefly, one day before transfection, CHOK1-SV cells were seeded at 0.5×10^6 cells/mL in 30 mL CD-CHO medium (Invitrogen) supplemented with 2 mM L-glutamine in 125 mL Erlenmeyer flasks (Corning). On the day of transfection, 20 μg DNA was diluted in OPTI-PRO SFM Medium (Invitrogen) and mixed with 200 μg PEI for 20 min at room temperature. The

DNA-PEI complexes were added to the cells, which were cultured in a CO_2 shaker incubator at 37°C, 135 rpm. After 72 hours, the expression of RIFINs and their recognition by the LAIR-1-containing antibodies were tested by flow cytometry. Briefly, 5 μg/mL of rabbit anti-HA tag and 2 μg/mL of MGC or MGD antibodies were added to the RIFIN-transfected cells. Antibody binding was detected by 5 μg/mL of Alexa Fluor 488-conjugated goat anti-rabbit IgG (Life Technologies, order number A11034) and 2.5 μg/mL of Alexa Fluor 647-conjugated goat anti-human IgG (Jackson ImmunoResearch, order number 109-606-170). Dead cells were excluded by staining with 7-AAD (BD Biosciences).

Inhibition of parasite growth. 3D7-MGD21$^+$ (5% parasitemia, ring stage) was cultured with various concentrations of MGD21 or BKC3 for 2 d. After 2 d, 10× SYBR Green I was added to aliquots of each culture and parasitemia was quantified by flow cytometry. The remaining parasites in each culture were washed to remove the antibodies and incubated for 1 d to allow the parasites to reach the late trophozoite/schizont stage. MGD21 recognition of these cultures was detected using 2.5 μg/mL of Alexa Fluor 647-conjugated goat anti-human IgG (Jackson ImmunoResearch, order number 109-606-107).

Inhibition of rosetting. 9605-MGD21$^+$ IE at the late trophozoite/schizont stage were purified from uninfected erythrocytes and ring-stage parasites using a magnetic column (Miltenyi Biotec) and resuspended in culture medium with 10% human serum. The purified IE were incubated with 10 μg/mL of MGD21 or BKC3 for 1 h at 4ºC, mixed with O^+ erythrocytes or A^+ erythrocytes in a 1:20 ratio, and incubated for 30 min at room temperature to allow rosetting to occur. The IE were stained with 10× SYBR Green I, and the number of rosettes formed by at least 200 IE was counted by fluorescence microscopy to calculate the rosetting rate.

Opsonic phagocytosis by monocytes. IE were stained with 10 μg/mL DAPI for 30 min at room temperature, washed four times and run on a magnetic column (Miltenyi Biotec) to purify late stage parasites. The purified parasites were opsonized with serially diluted antibodies for 1 h at 4ºC. Monocytes were isolated from fresh PBMCs of healthy donors using mouse anti-CD14 microbeads (Miltenyi, order number 130-050-201) and mixed with the opsonized parasites in a 1:2 ratio for 1 h at 37ºC. The cells were stained with

mouse anti-CD14-PE-Cy5 (Beckman Coulter, order number A07765) and analyzed by flow cytometry. The mean fluorescence intensity (MFI) of DAPI in $CD14^+$ cells was used as a measure of phagocytosis of IE by monocytes.

Statistics. The Wilcoxon signed-rank test was used for statistical comparisons of pairs of data groups in rosetting experiments.

References

1. Murray, C. J. L. *et al.* Global malaria mortality between 1980 and 2010: a systematic analysis. *Lancet* **379,** 413–431 (2012).
2. Chan, J.-A., Fowkes, F. J. I. & Beeson, J. G. Surface antigens of Plasmodium falciparum-infected erythrocytes as immune targets and malaria vaccine candidates. *Cell. Mol. Life Sci.* **71,** 3633–3657 (2014).
3. Scherf, A., Lopez-Rubio, J. J. & Riviere, L. Antigenic variation in Plasmodium falciparum. *Annu. Rev. Microbiol.* **62,** 445–470 (2008).
4. Rowe, J. A., Claessens, A., Corrigan, R. A. & Arman, M. Adhesion of Plasmodium falciparum-infected erythrocytes to human cells: molecular mechanisms and therapeutic implications. *Expert Rev Mol Med* **11,** e16 (2009).
5. Goel, S. *et al.* RIFINs are adhesins implicated in severe Plasmodium falciparum malaria. *Nat Med* **21,** 314–317 (2015).
6. Bull, P. C. *et al.* Parasite antigens on the infected red cell surface are targets for naturally acquired immunity to malaria. *Nat Med* **4,** 358–360 (1998).
7. Dodoo, D. *et al.* Antibodies to Variant Antigens on the Surfaces of Infected Erythrocytes Are Associated with Protection from Malaria in Ghanaian Children. *Infection and Immunity* **69,** 3713–3718 (2001).
8. Giha, H. A. *et al.* Antibodies to variable Plasmodium falciparum-infected erythrocyte surface antigens are associated with protection from novel malaria infections. *Immunol. Lett.* **71,** 117–126 (2000).
9. Biggs, B. A. *et al.* Antigenic variation in Plasmodium falciparum. *Proc Natl Acad Sci USA* **88,** 9171–9174 (1991).
10. Roberts, D. J. *et al.* Rapid switching to multiple antigenic and adhesive phenotypes in malaria. *Nature* **357,** 689–692 (1992).
11. Marsh, K. & Howard, R. J. Antigens induced on erythrocytes by P. falciparum: expression of diverse and conserved determinants. *Science* **231,** 150–153 (1986).
12. Iqbal, J., Perlmann, P. & Berzins, K. Serological diversity of antigens expressed on the surface of erythrocytes infected with Plasmodium falciparum. *Trans. R. Soc. Trop. Med. Hyg.* **87,** 583–588 (1993).
13. Newbold, C. I., Pinches, R., Roberts, D. J. & Marsh, K. Plasmodium falciparum: the human agglutinating antibody response to the infected red cell surface is predominantly variant specific. *Exp. Parasitol.* **75,** 281–292 (1992).
14. Chattopadhyay, R. *et al.* Plasmodium falciparum Infection Elicits Both Variant-Specific and Cross-Reactive Antibodies against Variant Surface Antigens. *Infection and Immunity* **71,** 597–604 (2003).
15. Traggiai, E. *et al.* An efficient method to make human monoclonal antibodies from memory B cells: potent neutralization of SARS coronavirus. *Nat. Med.* **10,** 871–875 (2004).
16. Meyaard, L. The inhibitory collagen receptor LAIR-1 (CD305). *Journal of Leukocyte Biology* **83,** 799–803 (2008).
17. Le Roch, K. G. *et al.* Discovery of gene function by expression profiling of the malaria parasite life cycle. *Science* **301,** 1503–1508 (2003).
18. Florens, L. *et al.* A proteomic view of the Plasmodium falciparum life cycle. *Nature* **419,** 520–526 (2002).
19. Abdel-Latif, M. S., Khattab, A., Lindenthal, C., Kremsner, P. G. & Klinkert, M. Q. Recognition of Variant Rifin Antigens by Human Antibodies Induced during

Natural Plasmodium falciparum Infections. *Infection and Immunity* **70,** 7013–7021 (2002).
20. Bachmann, A. *et al.* Temporal Expression and Localization Patterns of Variant Surface Antigens in Clinical Plasmodium falciparum Isolates during Erythrocyte Schizogony. *PLoS ONE* **7,** e49540–15 (2012).
21. Crompton, P. D. *et al.* Malaria immunity in man and mosquito: insights into unsolved mysteries of a deadly infectious disease. *Annu. Rev. Immunol.* **32,** 157–187 (2014).
22. Teng, G. *et al.* RAG Represents a Widespread Threat to the Lymphocyte Genome. *Cell* **162,** 751–765 (2015).
23. van der Vuurst de Vries, A. R., Clevers, H., Logtenberg, T. & Meyaard, L. Leukocyte-associated immunoglobulin-like receptor-1 (LAIR-1) is differentially expressed during human B cell differentiation and inhibits B cell receptor-mediated signaling. *Eur. J. Immunol.* **29,** 3160–3167 (1999).
24. Melek, M., Gellert, M. & van Gent, D. C. Rejoining of DNA by the RAG1 and RAG2 proteins. *Science* **280,** 301–303 (1998).
25. Messier, T. L., O'Neill, J. P. & Finette, B. A. V(D)J recombinase mediated inter-chromosomalHPRT alterations at cryptic recombination signal sequences in peripheral human T cells. *Hum. Mutat.* **27,** 829–829 (2006).
26. Han, S. *et al.* V(D)J recombinase activity in a subset of germinal center B lymphocytes. *Science* **278,** 301–305 (1997).
27. Messier, T. L., O'Neill, J. P., Hou, S.-M., Nicklas, J. A. & Finette, B. A. In vivo transposition mediated by V(D)J recombinase in human T lymphocytes. *EMBO J.* **22,** 1381–1388 (2003).
28. Vaandrager, J. W., Schuuring, E., Philippo, K. & Kluin, P. M. V(D)J recombinase-mediated transposition of the BCL2 gene to the IGH locus in follicular lymphoma. *Blood* **96,** 1947–1952 (2000).
29. Küppers, R. & Dalla-Favera, R. Mechanisms of chromosomal translocations in B cell lymphomas. *Oncogene* **20,** 5580–5594 (2001).
30. Küppers, R., Klein, U., Hansmann, M. L. & Rajewsky, K. Cellular origin of human B-cell lymphomas. *N Engl J Med* **341,** 1520–1529 (1999).
31. Robbiani, D. F. *et al.* Plasmodium Infection Promotes Genomic Instability and AID-Dependent B Cell Lymphoma. *Cell* **162,** 727–737 (2015).
32. Nemazee, D. & Weigert, M. Revising B cell receptors. *Journal of Experimental Medicine* **191,** 1813–1817 (2000).
33. Sabouri, Z. *et al.* Redemption of autoantibodies on anergic B cells by variable-region glycosylation and mutation away from self-reactivity. *Proc Natl Acad Sci USA* **111,** E2567–E2575 (2014).
34. Zhou, T. *et al.* Structural basis for broad and potent neutralization of HIV-1 by antibody VRC01. *Science* **329,** 811–817 (2010).
35. Holmdahl, R., Malmström, V. & Burkhardt, H. Autoimmune priming, tissue attack and chronic inflammation - the three stages of rheumatoid arthritis. *Eur. J. Immunol.* **44,** 1593–1599 (2014).
36. Brondijk, T. H. C. *et al.* Crystal structure and collagen-binding site of immune inhibitory receptor LAIR-1: unexpected implications for collagen binding by platelet receptor GPVI. *Blood* **115,** 1364–1373 (2010).
37. Cox, J. & Mann, M. MaxQuant enables high peptide identification rates, individualized p.p.b.-range mass accuracies and proteome-wide protein

quantification. *Nature Biotechnology* **26,** 1367–1372 (2008).
38. Schwanhäusser, B. *et al.* Global quantification of mammalian gene expression control. *Nature* **473,** 337–342 (2011).
39. Trager, W. & Jensen, J. B. Human malaria parasites in continuous culture. *Science* **193,** 673–675 (1976).
40. Tiller, T. *et al.* Efficient generation of monoclonal antibodies from single human B cells by single cell RT-PCR and expression vector cloning. *Journal of Immunological Methods* **329,** 112–124 (2008).
41. Lefranc, M.-P. *et al.* IMGT, the international ImMunoGeneTics information system. *Nucleic Acids Research* **37,** D1006–12 (2009).
42. Larkin, M. A. *et al.* Clustal W and Clustal X version 2.0. *Bioinformatics* **23,** 2947–2948 (2007).
43. Merelli, I. *et al.* RSSsite: a reference database and prediction tool for the identification of cryptic Recombination Signal Sequences in human and murine genomes. *Nucleic Acids Research* **38,** W262–7 (2010).
44. Kepler, T. B. Reconstructing a B-cell clonal lineage. I. Statistical inference of unobserved ancestors. *F1000Res* **2,** 103 (2013).
45. Liao, H.-X. *et al.* Co-evolution of a broadly neutralizing HIV-1 antibody and founder virus. *Nature* **496,** 469–476 (2013).
46. Pappas, L. *et al.* Rapid development of broadly influenza neutralizing antibodies through redundant mutations. *Nature* **516,** 418–422 (2014).

Acknowledgements We would like to thank M. Nussenzweig and H. Wardemann for providing reagents for antibody cloning and expression. This work was supported by the European Research Council (grant no. 250348 IMMUNExplore), the Swiss National Science Foundation (grant no. 141254) and the Wellcome Trust (grant no. 084535, 077092 and 084538). J.T. is funded by the Wellcome Trust (grant no. 099811). A.L. is supported by the Helmut Horten Foundation. This paper is published with the permission of the Director of KEMRI.

Author Contributions J.T. performed all experiments involving *P. falciparum*, analysed the data and wrote the manuscript; K.P. characterized genomic DNA, analysed the data and wrote the manuscript; L.P. produced mutant antibodies, analysed the data and wrote the manuscript; A.A. set up parasite cultures; C.M.T. made initial observations of mixed agglutination; M.F.P. performed bioinformatics analysis; R.G. analysed MS data; D.J. performed sorting and analysed the data; F.M.N., J.W. and P.Be. provided cohort samples; C.S.F. performed B cell immortalization; B.F-R. and S.Ba. sequenced and expressed antibodies; S.Bi. performed IP experiments; K.M., V.T., D.C. and F.S.

provided supervision; A.L. and P.Bu. provided overall supervision, analysed the data and wrote the manuscript.

Author Information Reprints and permissions information is available at www.nature.com/reprints. A.L. is the scientific founder and shareholder of Humabs BioMed. F.S. is a shareholder of Humabs BioMed. S.Bi. and D.C. are employees of Humabs BioMed, a company that commercializes human monoclonal antibodies. Correspondence and requests for materials should be addressed to A.L. (lanzavecchia@irb.usi.ch) or P.Bu. (PBull@kemri-wellcome.org).

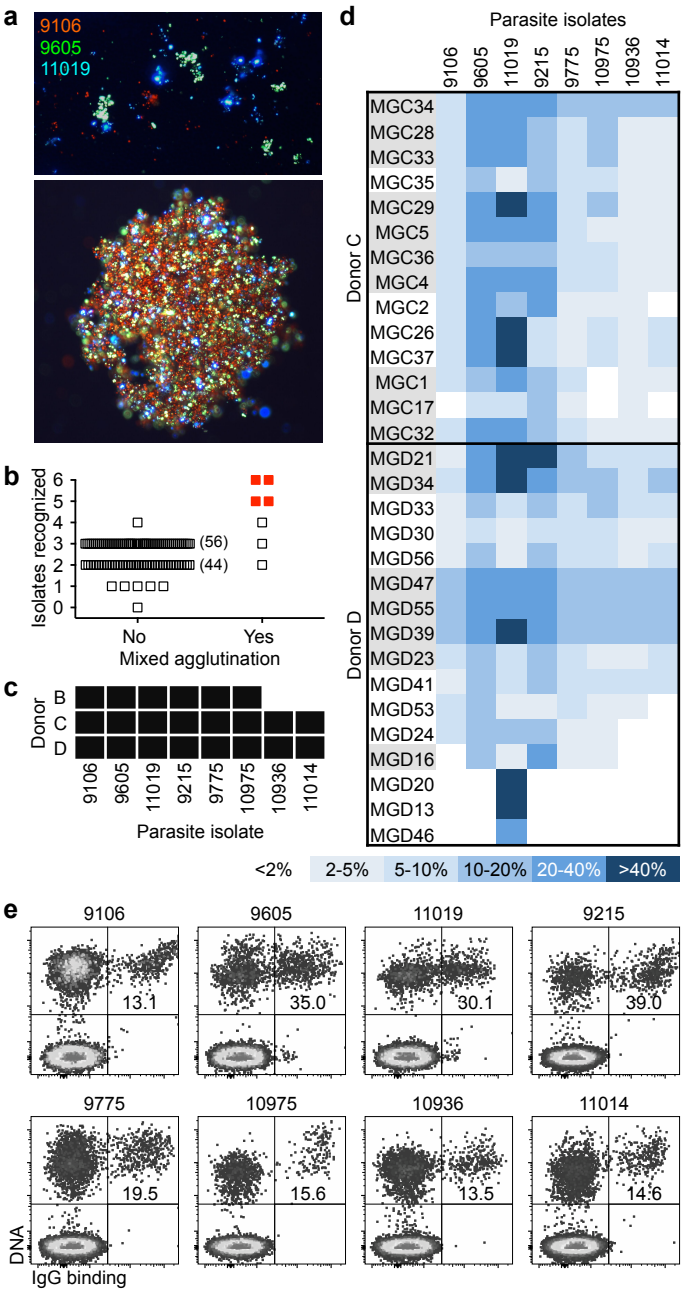
a
9106
9605
11019
b
Isolates recognized
6
5
4
3
2
1
0
(56)
(44)
No
Yes
Mixed agglutination
c
Donor
B
C
D
9106
9605
11019
9215
9775
10975
10936
11014
Parasite isolate
d
Parasite isolates
9106
9605
11019
9215
9775
10975
10936
11014
Donor C
MGC34
MGC28
MGC33
MGC35
MGC29
MGC5
MGC36
MGC4
MGC2
MGC26
MGC37
MGC1
MGC17
MGC32
Donor D
MGD21
MGD34
MGD33
MGD30
MGD56
MGD47
MGD55
MGD39
MGD23
MGD41
MGD53
MGD24
MGD16
MGD20
MGD13
MGD46
<2%
2-5%
5-10%
10-20%
20-40%
>40%
e
9106
9605
11019
9215
13.1
35.0
30.1
39.0
9775
10975
10936
11014
19.5
15.6
13.5
14.6
DNA
IgG binding

Figure 1

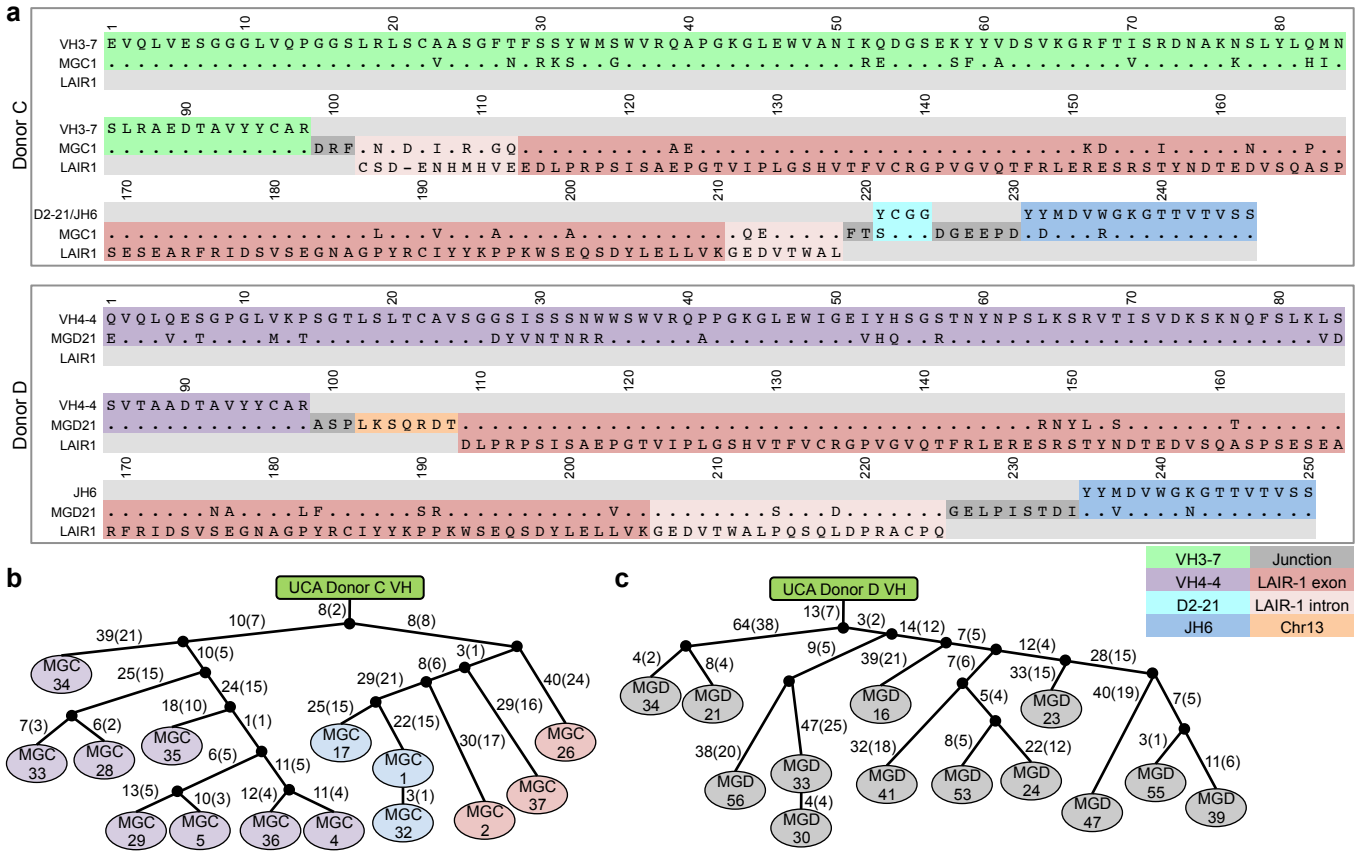
a
Donor C
VH3-7
MGC1
LAIR1
D2-21/JH6
Donor D
VH4-4
MGD21
JH6
b
UCA Donor C VH
c
UCA Donor D VH
VH3-7
VH4-4
D2-21
JH6
Junction
LAIR-1 exon
LAIR-1 intron
Chr13

Figure 2

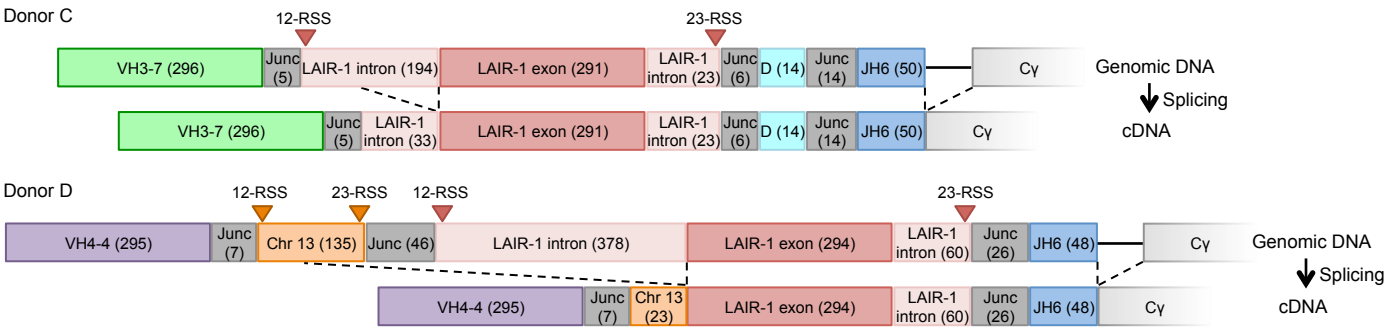
Donor C
12-RSS
23-RSS
VH3-7 (296)
Junc (5)
LAIR-1 intron (194)
LAIR-1 exon (291)
LAIR-1 intron (23)
Junc (6)
D (14)
Junc (14)
JH6 (50)
Cγ
Genomic DNA
Splicing
cDNA
VH3-7 (296)
Junc (5)
LAIR-1 intron (33)
LAIR-1 exon (291)
LAIR-1 intron (23)
Junc (6)
D (14)
Junc (14)
JH6 (50)
Cγ
Donor D
12-RSS
23-RSS
12-RSS
23-RSS
VH4-4 (295)
Junc (7)
Chr 13 (135)
Junc (46)
LAIR-1 intron (378)
LAIR-1 exon (294)
LAIR-1 intron (60)
Junc (26)
JH6 (48)
Cγ
Genomic DNA
Splicing
cDNA
VH4-4 (295)
Junc (7)
Chr 13 (23)
LAIR-1 exon (294)
LAIR-1 intron (60)
Junc (26)
JH6 (48)
Cγ

Figure 3

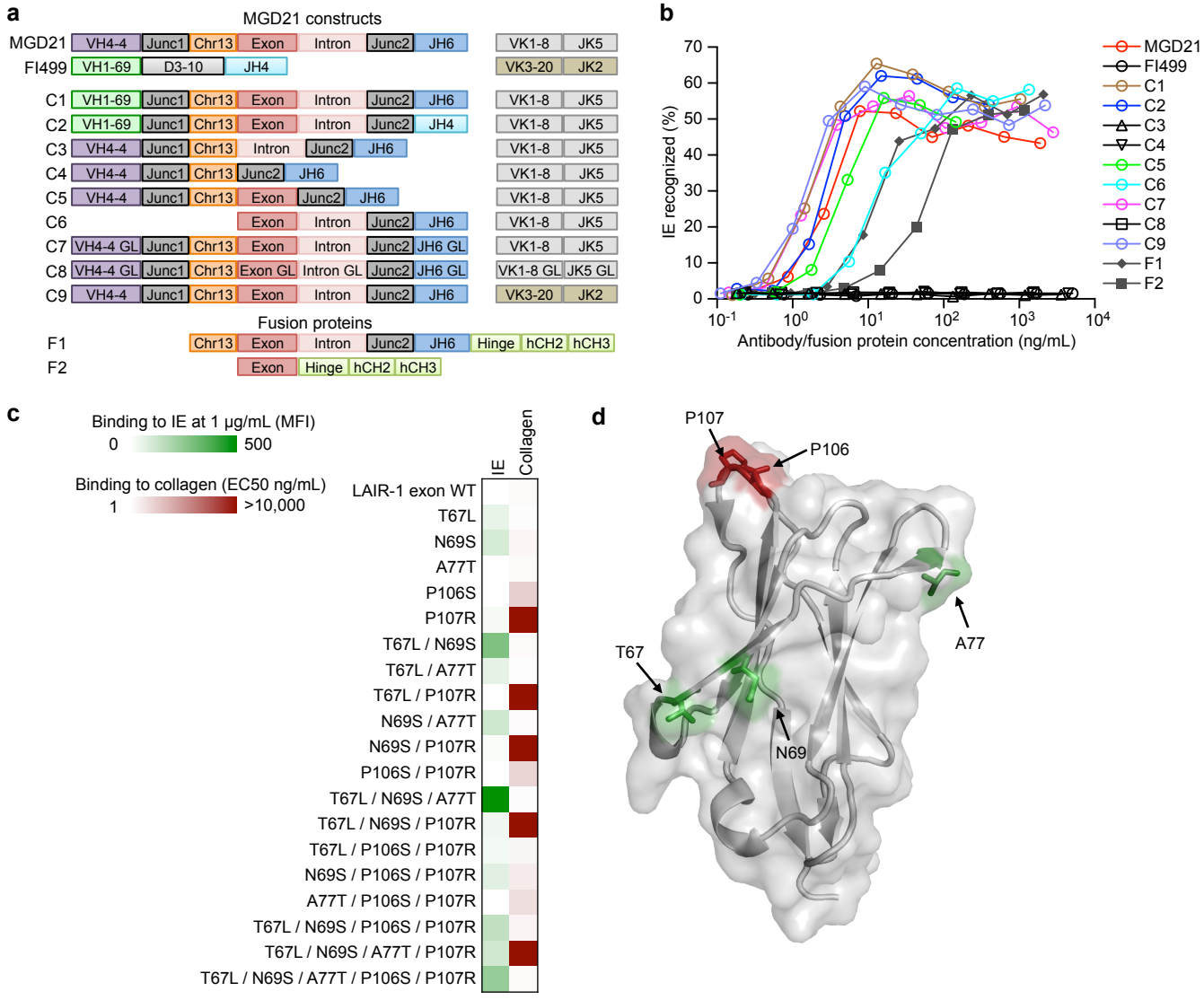
a
MGD21 constructs
MGD21
FI499
C1
C2
C3
C4
C5
C6
C7
C8
C9
F1
F2
VH4-4
VH1-69
VH4-4 GL
Junc1
Chr13
Exon
Intron
Junc2
JH6
JH4
D3-10
VK1-8
VK3-20
VK1-8 GL
JK5
JK2
JK5 GL
Exon GL
Intron GL
JH6 GL
Fusion proteins
Hinge
hCH2
hCH3
b
IE recognized (%)
Antibody/fusion protein concentration (ng/mL)
c
Binding to IE at 1 µg/mL (MFI)
0
500
Binding to collagen (EC50 ng/mL)
1
>10,000
IE
Collagen
LAIR-1 exon WT
T67L
N69S
A77T
P106S
P107R
T67L / N69S
T67L / A77T
T67L / P107R
N69S / A77T
N69S / P107R
P106S / P107R
T67L / N69S / A77T
T67L / N69S / P107R
T67L / P106S / P107R
N69S / P106S / P107R
A77T / P106S / P107R
T67L / N69S / P106S / P107R
T67L / N69S / A77T / P107R
T67L / N69S / A77T / P106S / P107R
d
P107
P106
T67
A77
N69

Figure 4

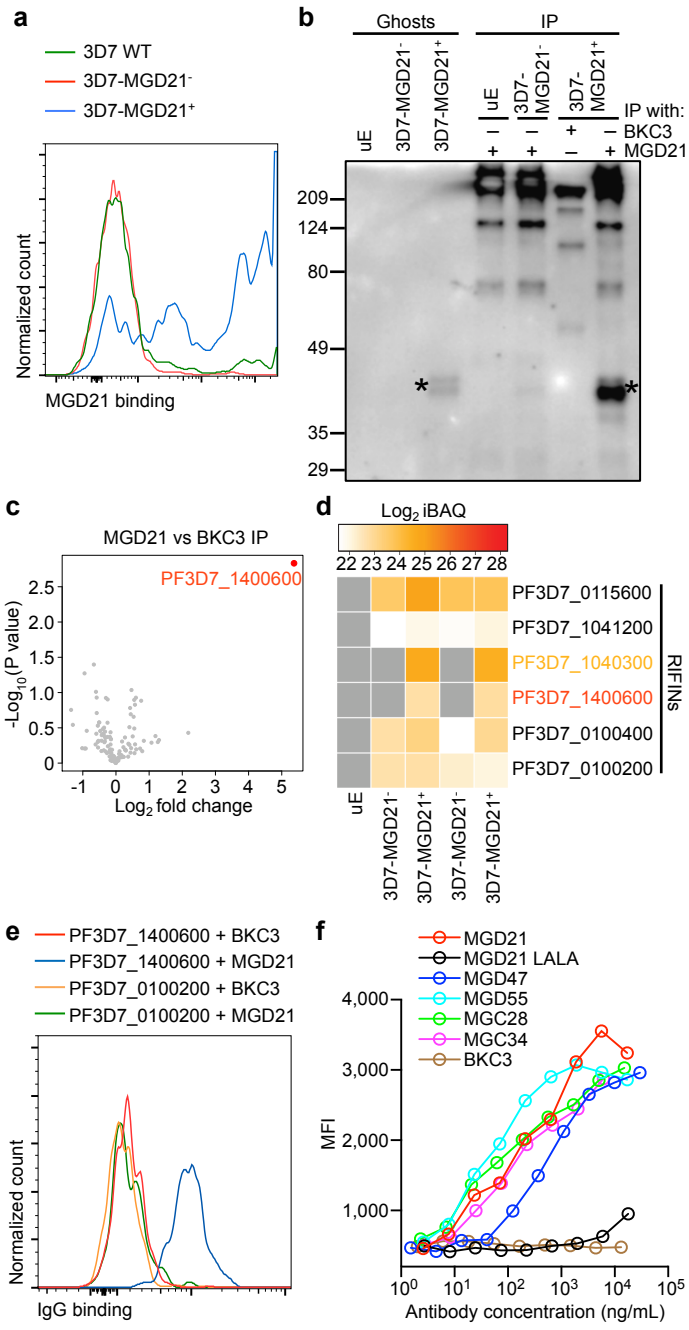
a
3D7 WT
3D7-MGD21-
3D7-MGD21+
Normalized count
MGD21 binding
b
Ghosts
IP
uE
3D7-MGD21-
3D7-MGD21+
IP with:
BKC3
MGD21
209
124
80
49
35
29
c
MGD21 vs BKC3 IP
PF3D7_1400600
-Log10(P value)
Log2 fold change
d
Log2 iBAQ
22 23 24 25 26 27 28
PF3D7_0115600
PF3D7_1041200
PF3D7_1040300
PF3D7_1400600
PF3D7_0100400
PF3D7_0100200
RIFINs
e
PF3D7_1400600 + BKC3
PF3D7_1400600 + MGD21
PF3D7_0100200 + BKC3
PF3D7_0100200 + MGD21
Normalized count
IgG binding
f
MGD21
MGD21 LALA
MGD47
MGD55
MGC28
MGC34
BKC3
MFI
Antibody concentration (ng/mL)

Figure 5

a Donor C

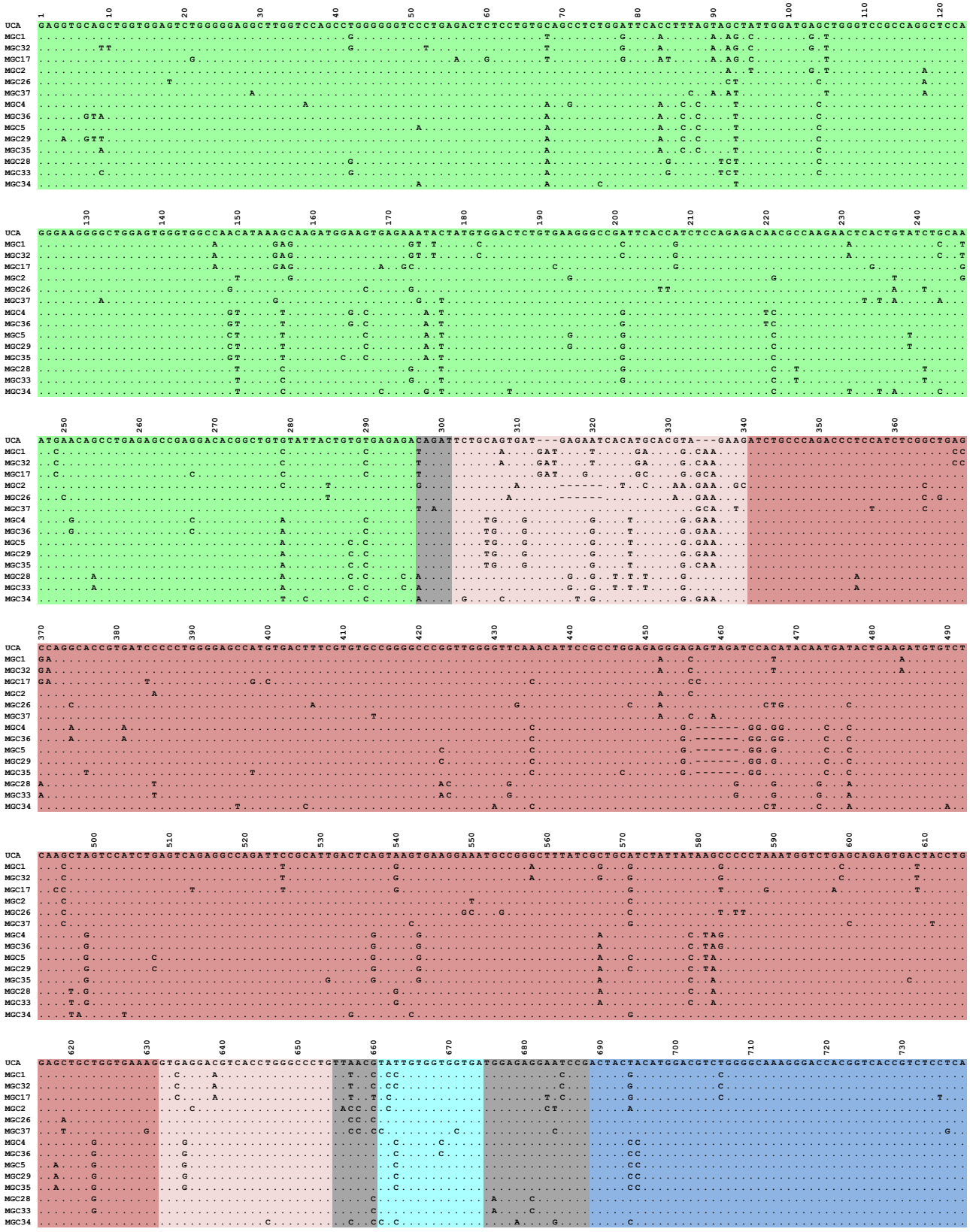

Extended Data Figure 1

b Donor D

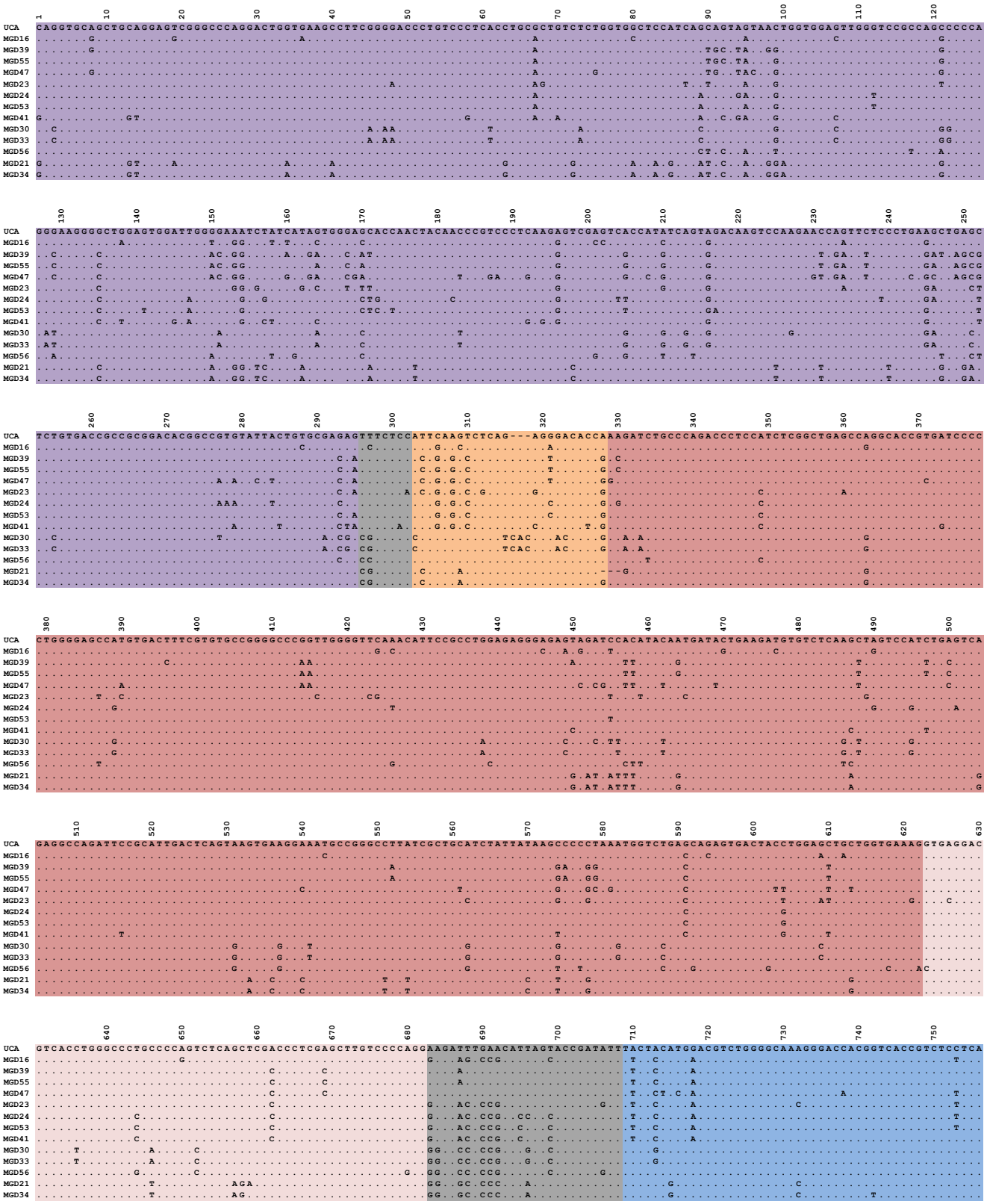

Extended Data Figure 1 (continued)

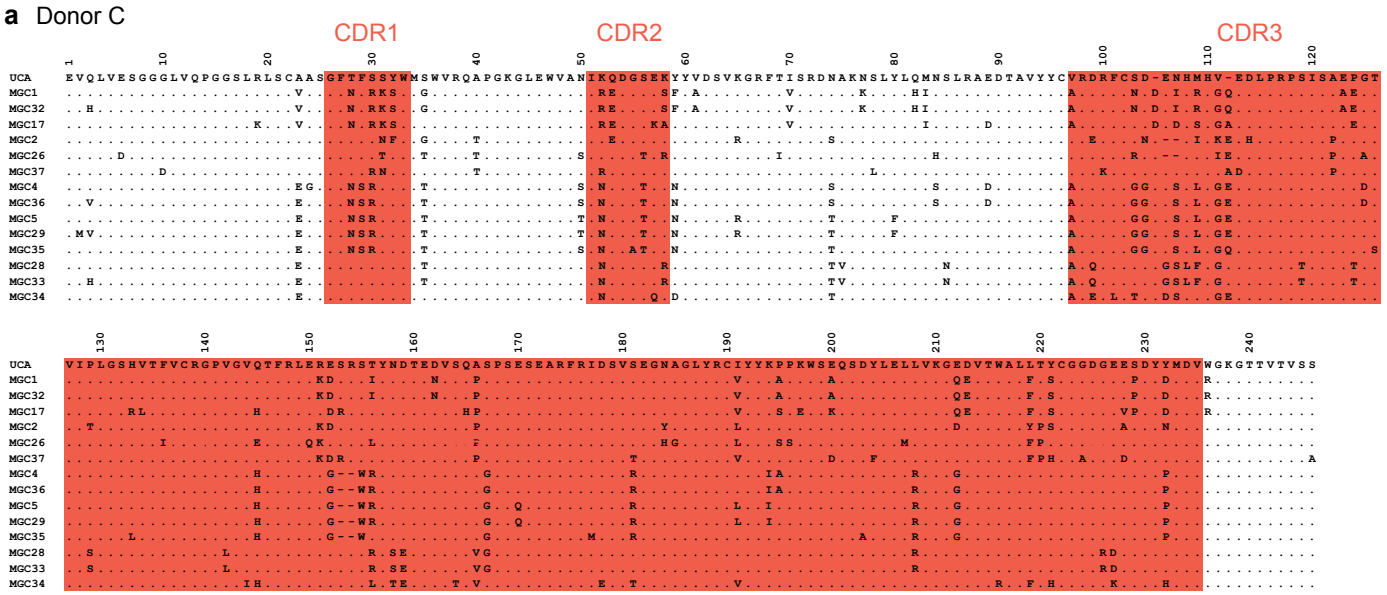

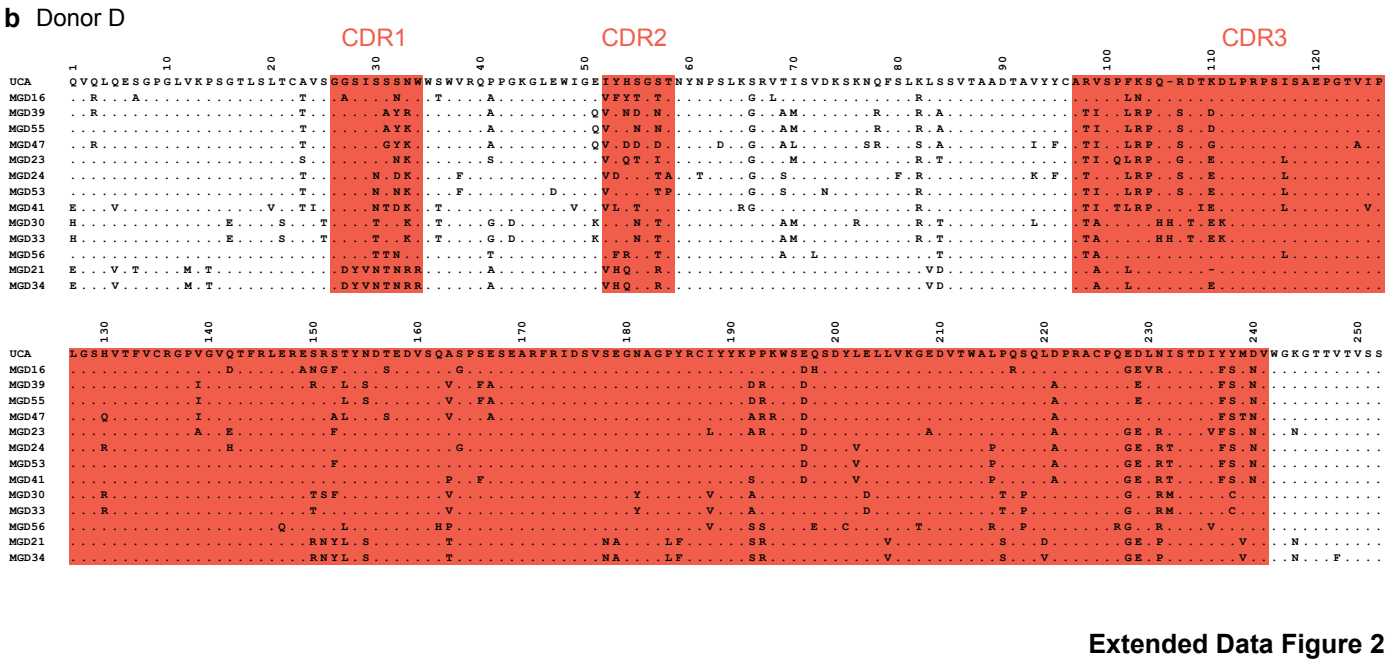

Extended Data Figure 2

a Donor C: VL7-43/JL3

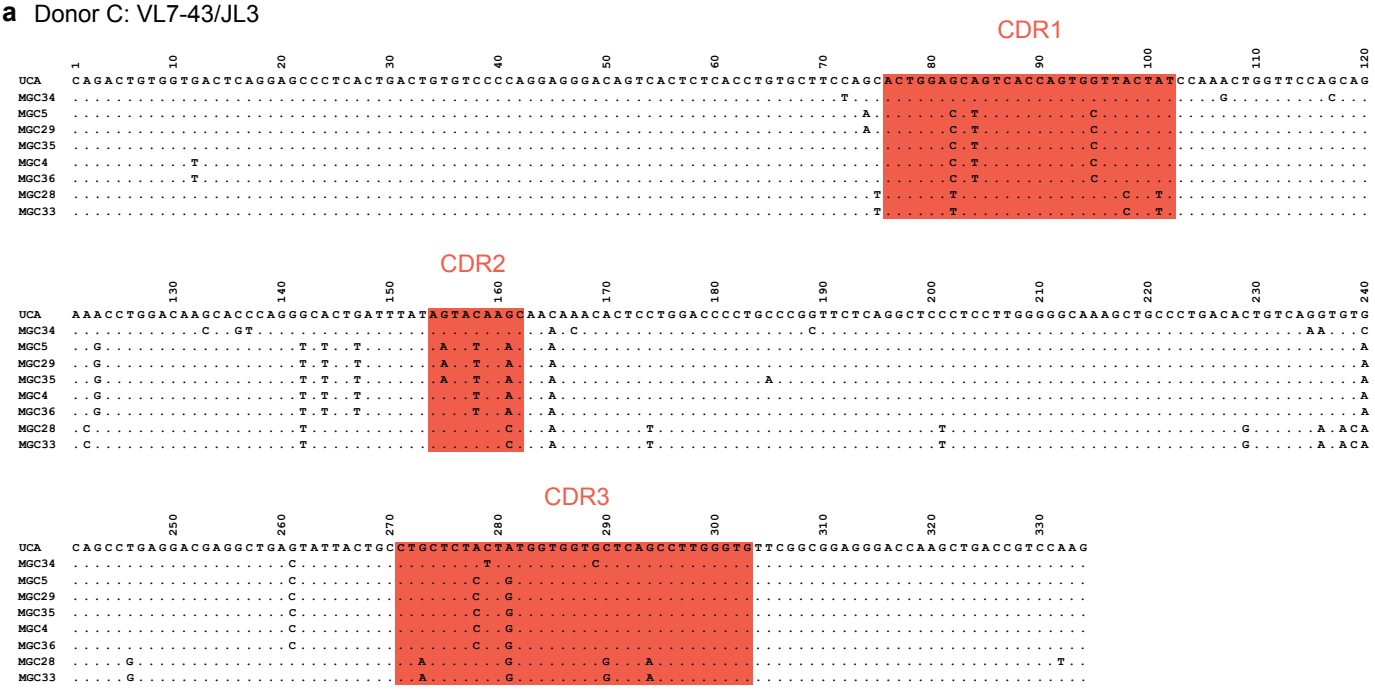

b Donor C: VK4-1/JK2

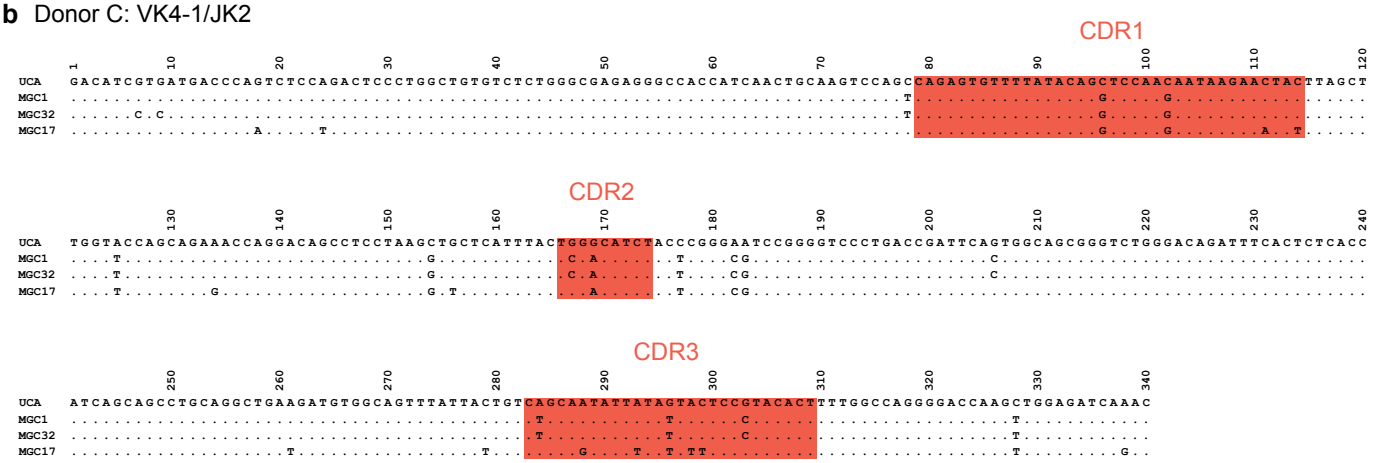

c Donor C: VK1-5/JK2

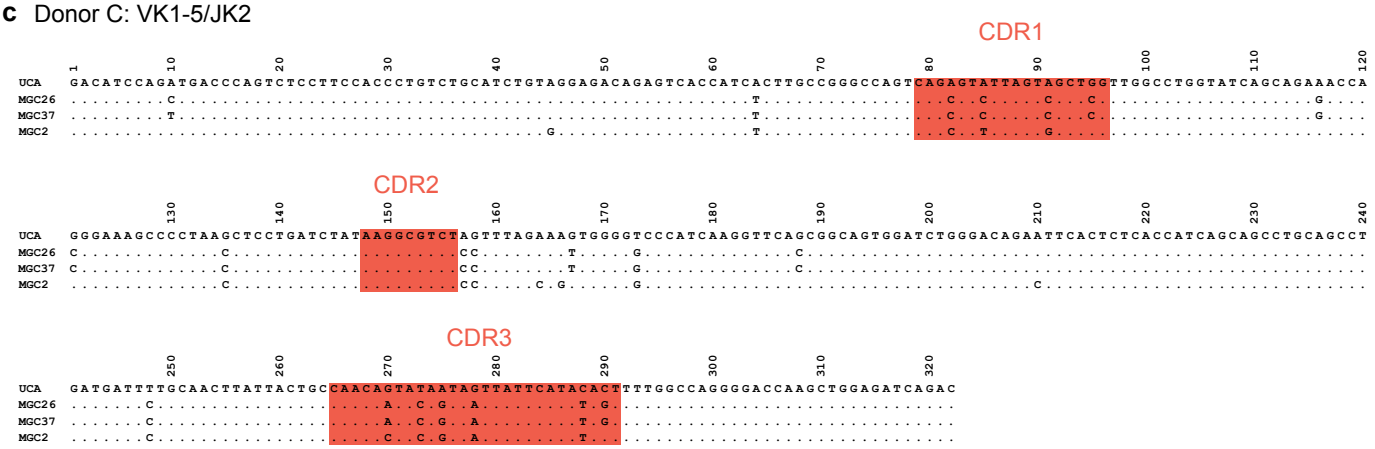

Extended Data Figure 3

d Donor D: VK1-8/JK5

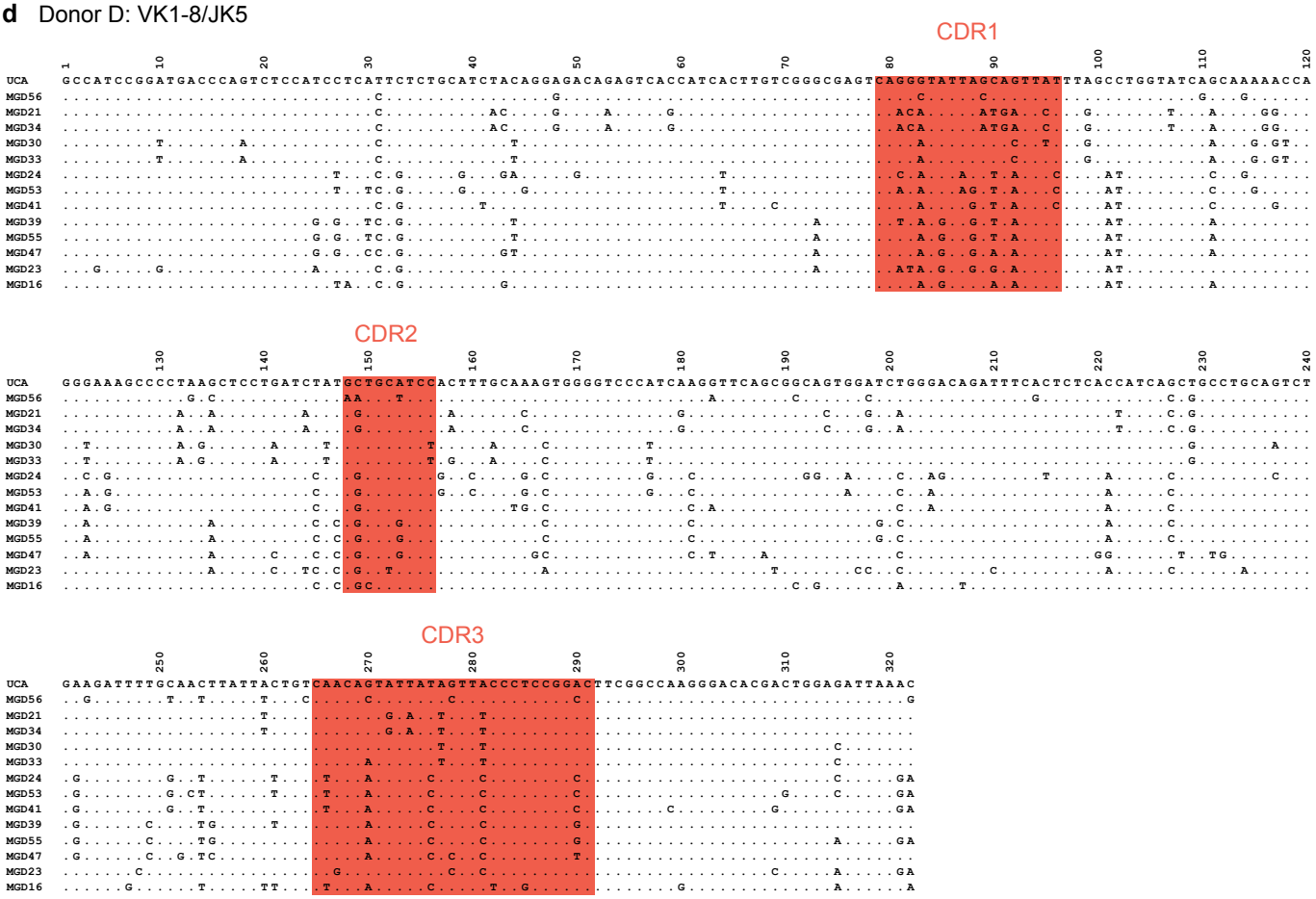

Extended Data Figure 3 (continued)

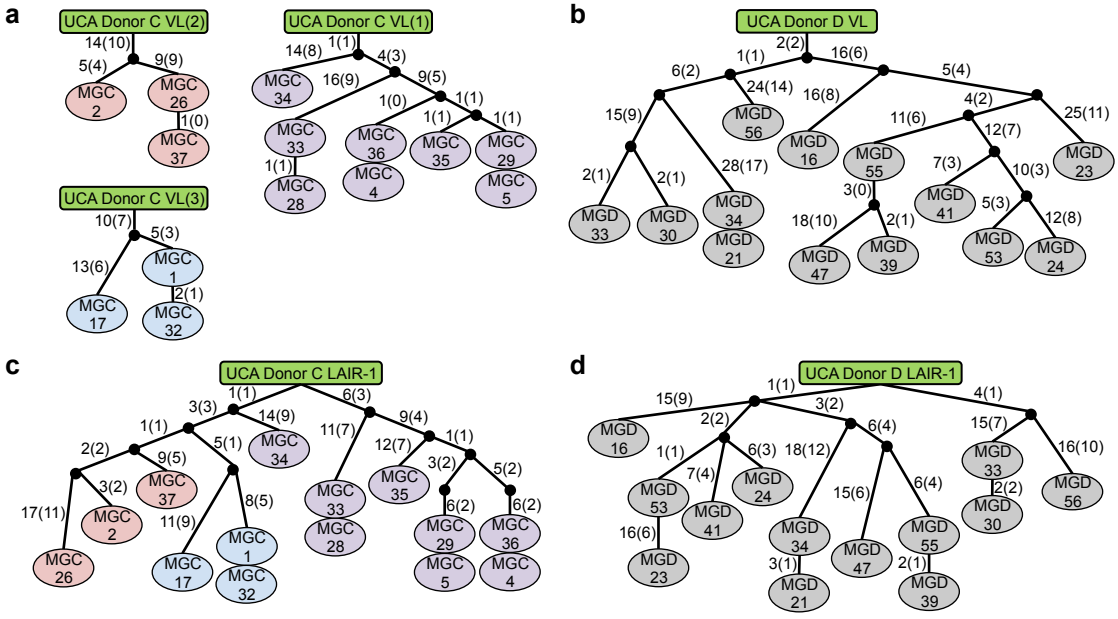

Extended Data Figure 4

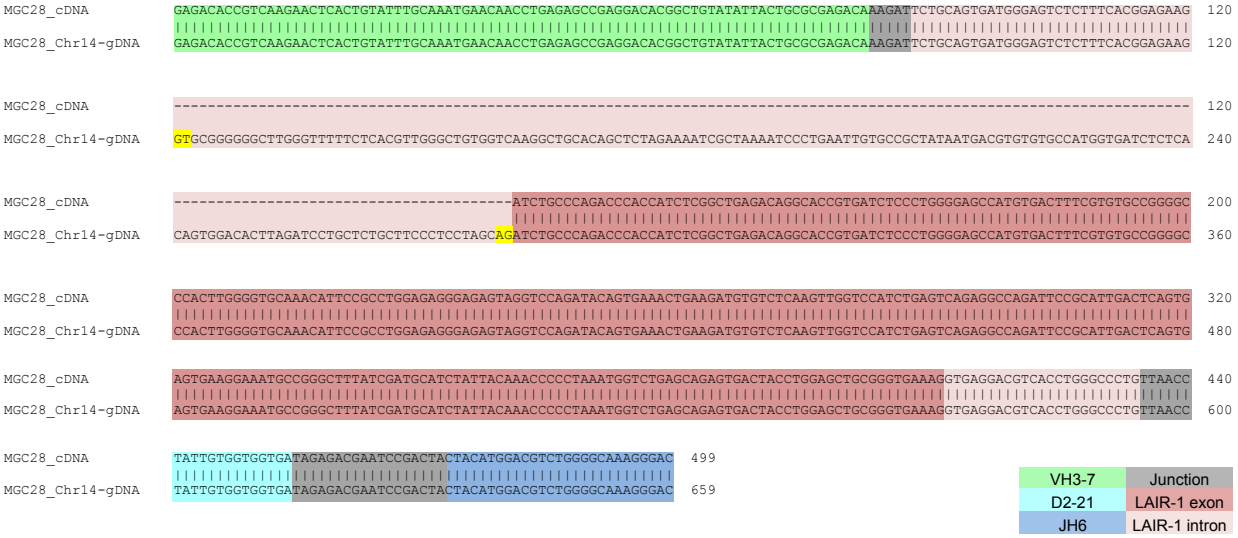

Extended Data Figure 5

Extended Data Figure 6

Extended Data Figure 7

	IE		RIFIN-transfected CHO cells				
	3D7-MGD21^{-}	3D7-MGD21^{+}	PF3D7_1400600	PF3D7_1040300	PF3D7_0100400	PF3D7_0100200	PF3D7_1100500
MGD21	3.4	54.2	46.7	22.2	1.7	0.4	1.3
MGD39	2.8	58.0	18.6	44.2	0.8	3.1	2.1
MGD47	3.5	55.3	6.0	2.2	1.2	1.9	2.7
MGD55	4.2	61.3	3.7	48.6	0.4	0.4	1.1
MGC1	0.9	7.1	0.5	0.4	0.3	1.0	0.0
MGC2	0.3	0.9	0.0	0.5	0.2	0.0	1.5
MGC4	0.6	0.8	0.3	1.8	0.0	1.0	0.0
MGC5	0.8	0.9	0.0	0.0	0.9	0.0	0.0
MGC17	0.4	0.7	1.3	0.8	0.6	1.3	1.4
MGC26	0.9	0.5	1.1	0.0	0.3	0.4	1.4
MGC28	1.8	42.4	0.9	51.9	0.3	0.5	2.4
MGC29	0.3	0.8	1.2	1.2	0.5	0.0	4.2
MGC34	1.9	48.8	3.4	6.4	1.4	2.0	3.3
BKC3	0.7	0.3	0.7	1.7	0.2	0.0	0.0

IE or CHO cells recognized (%)

0 50

Extended Data Figure 8

a

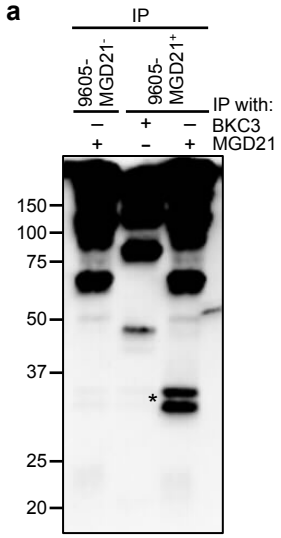

b

	9605-MGD21^{-}	9605-MGD21^{+}
MGD21	10.9	37.3
MGD39	15.6	38.2
MGD47	19.6	37.9
MGD55	21.5	37.8
MGC1	14.6	26.3
MGC2	13.3	34.0
MGC4	9.8	31.6
MGC5	7.1	29.7
MGC17	12.0	28.1
MGC26	15.9	29.2
MGC28	9.9	34.5
MGC29	10.2	34.5
MGC34	10.7	32.4
BKC3	3.2	3.4

IE recognized (%)
0 50

Extended Data Figure 9

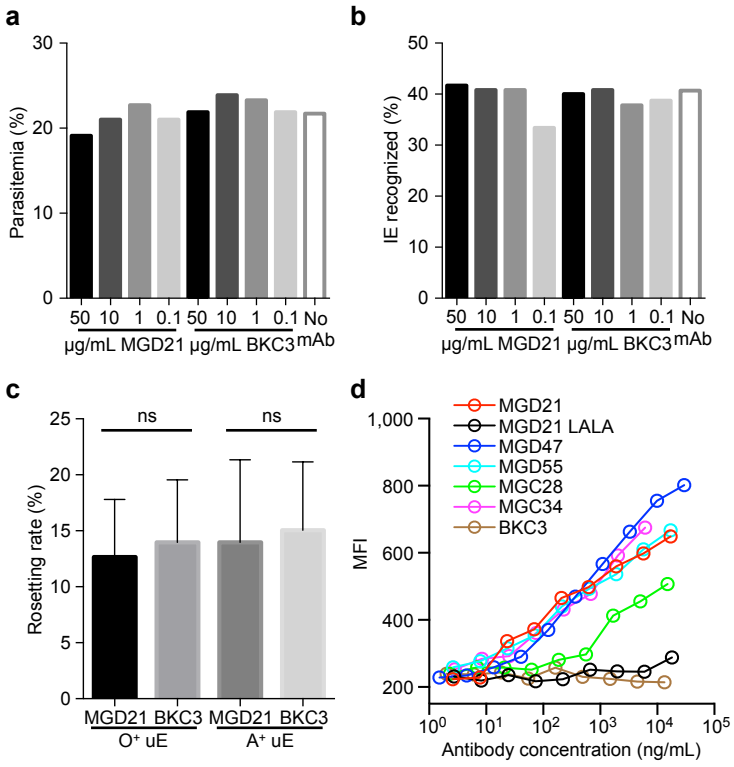

Extended Data Figure 10